Supplementary Information: Dimension reducing structural transformation in monolayer materials: 2D to 1D transformations

Kasra Momeni*, Hamed Attariani, Richard A LeSar

Supplementary Figures

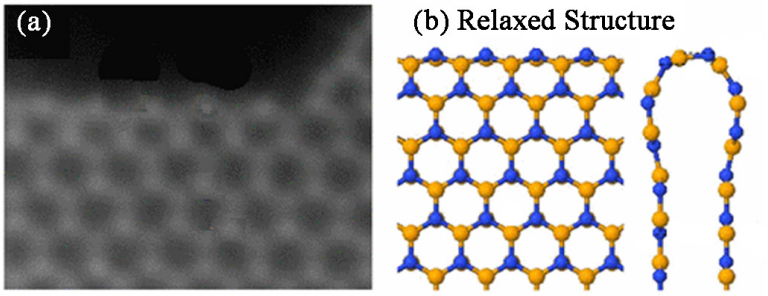

Supplementary Figure 1. Experimental evidence for the formation of a half monolayer nanodumbbell structure at the free standing edges of hexagonal Boron Nitride (h-BN). (a) The high resolution transmission electron microscopy image of the structure at the edges of a bi-layer h-BN; (b) Corresponding schematic of the plane and cross-sectional views of relaxed atomic structure indicating formation of a half monolayer nanodumbbell like structure. Reprinted from Ref. [1] with permission.

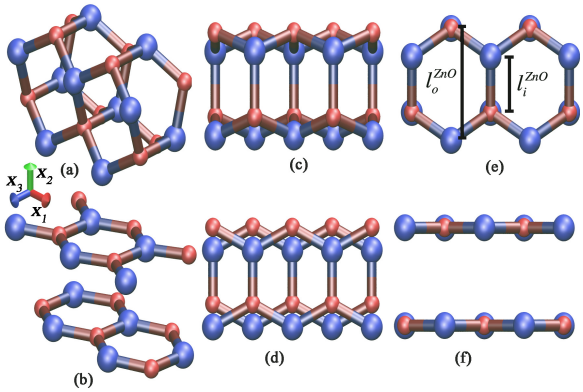

Supplementary Figure 2. Crystal structure of the ZnO nanoribbon before and after nanoribbon to monolayer nanodumbbell transformation. (a, b) the 3D view, (c, d) top view, and (e, f) side view of two unit cells in a nanoribbon before structural transformation (top row) and after structural transformation (bottom row). The l_o^{ZnO} and l_i^{ZnO} represent the distance between two outer and inner Zn-O atoms in the unrelaxed crystalline structure, respectively. The distance between two succeeding zinc (oxygen) atoms in $(\bar{1}100)$ surfaces is 3.265 Å. The distance between Zn-O in the $(11\bar{2}0)$, at the outer and inner $(\bar{1}100)$ surfaces are $l_o^{ZnO} = 3.77$ Å and $l_i^{ZnO} = 1.885$ Å, respectively.

* kzm5606@psu.edu

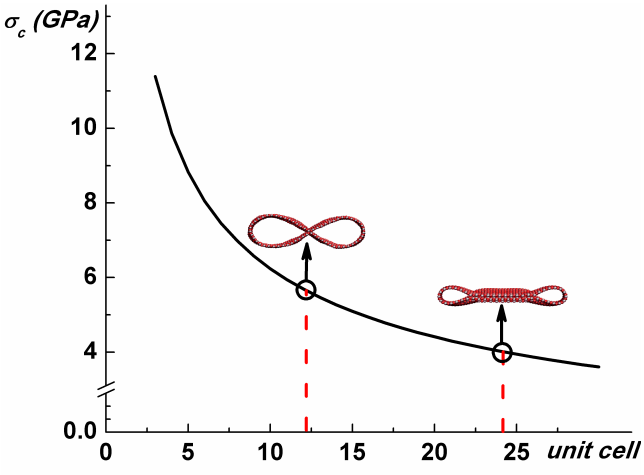

Supplementary Figure 3. Induced compressive stress due to surface tension. The compressive stress induced in the core of a nanoribbon as a function of number of unit cells in the width. Maximum number of unit cells for the formation of nanotube is 11 resulting in 5.95 GPa stress in the core of nanoribbon, which is almost equal to the 6.0 GPa stress reported for wurtzite to graphite-like ZnO. The minimum number of unit cells for the formation of monolayer nanodumbbell is 24 that result in 4.03 GPa.

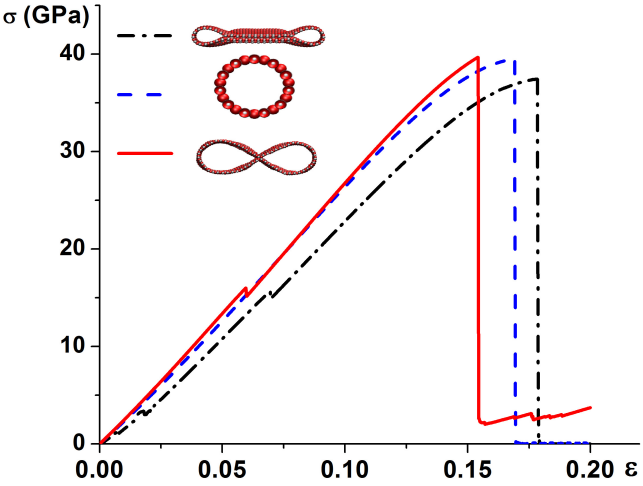

Supplementary Figure 4. Uniaxial stress-strain curve of ZnO nanostructures. Uniaxial loading is performed along [0001] direction for monolayer nanodumbbell (dash-dotted line), nanotube (dashed line), and twin-nanotube (solid line). The elastic modulus of the twin-nanotube, nanotube, and monolayer nanodumbbell are calculated as the slope of the linear part of the graph as 247.3 GPa, 231.8 GPa, and 171.25 GPa, respectively.

MATERIALS AND METHODS

We considered a Coulomb–Buckingham potential for ZnO [2] and GaN [3] that is presented in eq. (A.1) and its parameters are listed in the Supplementary table I. A rigid ion approximation was assumed that neglects the effect of polarization between the massive positively-charged

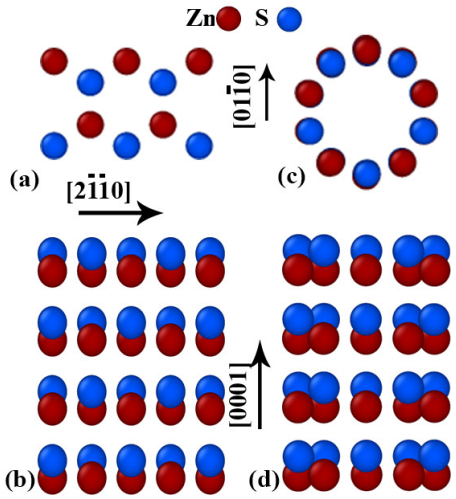

Supplementary Figure 5. Nanosheet to NT structural transformation for a ZnS nanosheet with 2 unit cells along the $[2\bar{1}\bar{1}0]$ direction. (a, b) structure of nanosheet before transformation; (c, d) structure of the final NT formed after transformation. Periodic boundary conditions are considered with 29 unitcells in the primary simulation cell along the [0001] direction, which are not shown here for conciseness.

nucleus and the massless negatively-charged electron gas. This model is computationally efficient without overly sacrificing accuracy. [4] The total Coloumb–Buckingham potential is

$$E\left(r_{ij}\right) = \frac{q_i q_j}{r_{ij}} + A\exp\left(-r_{ij}/\rho\right) - \frac{C}{r_{ij}^6}, \tag{A.1}$$

where r_{ij} is the distance between two ions; A, C, and ρ are parameters that specify the simulated material (Supplementary I); and q_i is the charge of i'th ion.

For ZnS, a Coulomb–Three-body potential is used,

$$E(r_{ij}) = \frac{q_i q_j}{r_{ij}} + A\,\exp\left(-r_{ij}/\rho\right) - \frac{C}{r_{ij}^6} + \frac{1}{2}K\,\left(\theta_{ijk} - \theta_0\right)^2 \tag{A.2}$$

where, K is the spring constant for the three-body potential and θ_0 is the equilibrium angle between S-Zn-S. Parameters for this potential are listed in the Supplementary II.

The velocity of the atoms were initialized using Boltzmann distribution. Long-range electrostatic interactions were calculated using the Wolf summation. [5,6] An infinite length of nanoribbon is modeled using periodic boundary conditions along the c-axis, while free boundary conditions were assumed for the other two directions. The open source MD simulation software package LAMMPS [7] was utilized for performing the simulations. The temperature

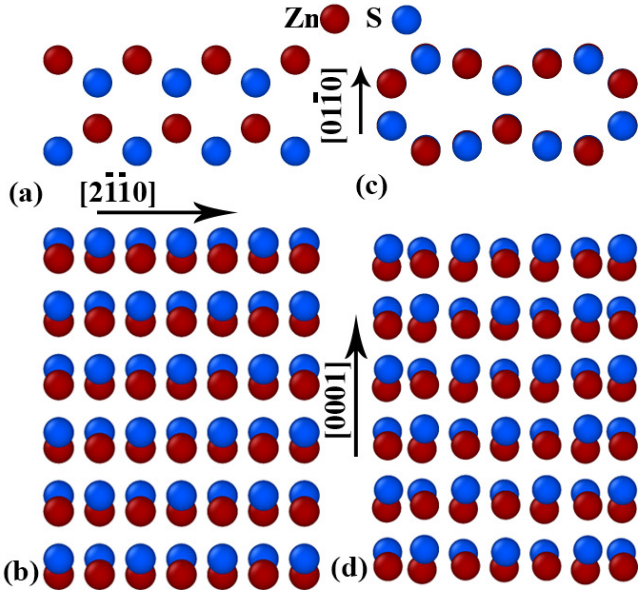

Supplementary Figure 6. Nanosheet to twin NT structural transformation for a ZnS nanosheet with 3 unit cells along the $[2\bar{1}\bar{1}0]$ direction. (a, b) structure of nanosheet before transformation; (c, d) structure of the final twin NT formed after transformation. Periodic boundary conditions are considered with 29 unitcells in the primary simulation cell along the [0001] direction, which are not shown here for conciseness.

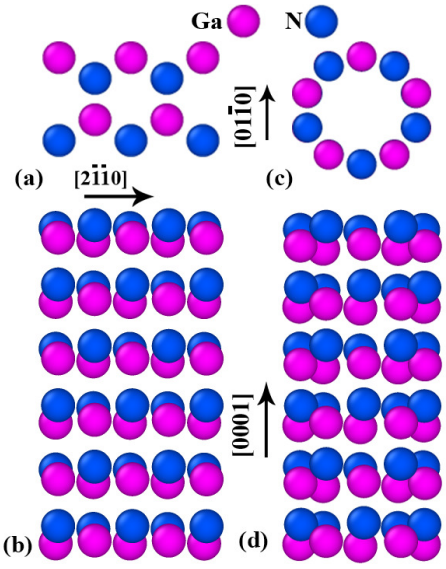

Supplementary Figure 7. Nanosheet to NT structural transformation for a GaN nanosheet with 2 unit cells along the $[2\bar{1}\bar{1}0]$ direction. (a, b) structure of nanosheet before transformation; (c, d) structure of the final NT formed after transformation. Periodic boundary conditions are considered with 29 unitcells in the primary simulation cell along the [0001] direction, which are not shown here for conciseness.

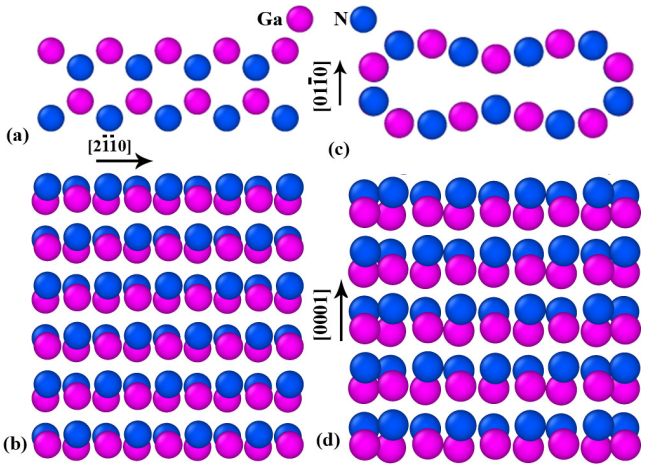

Supplementary Figure 8. Nanosheet to twin NT structural transformation for a GaN nanosheet with 5 unit cells along the [2$\bar{1}\bar{1}$0] direction. (a, b) structure of nanosheet before transformation; (c, d) structure of the final twin NT formed after transformation. Periodic boundary conditions are considered with 29 unitcells in the primary simulation cell along the [0001] direction, which are not shown here for conciseness.

scaling method is used in the NVE ensemble, while Nose-Hoover barostat is utilized for the NPT simulations. A cut-off radius of 1 nm is assumed for the Buckingham and coulomb parts of the energy along with a damping coefficient of $\alpha = 0.4$ in the Wolf summation to avoid convergence problems. [8]

Supplementary Table I. Parameters of the Coulomb–Buckingham potential of ZnO [2] and GaN [3] for a rigid ion model.

Ions	A (eV)	ρ (Å)	C(eV^{-6})
$O^{2-} - O^{2-}$	9547.096	0.21916	32.0
$Zn^{2+} - Zn^{2+}$	0.0	0.0	0.0
$Zn^{2+} - O^{2-}$	529.70	0.3581	0.0
$Ga^{3+} - Ga^{3+}$	6068.14	0.31846	250.0
$N^{3-} - N^{3-}$	4115.42	0.31949	280.0
$Ga^{3+} - N^{3-}$	872.42	0.31318	0.0

The nanostructures were relaxed for 1 ns using NVE ensemble and temperature scaling method with free boundary conditions. It was followed by relaxation in NPT ensemble at specified temperatures without any external pressure for 49 ns, using a Nose-Hoover barostat.

Supplementary Table II. Parameters of the Coulomb–Three-body potential of ZnS [9] for a rigid ion model.

Ions	A (eV)	ρ (Å)	C(eV^{-6})
$S^{2-} - S^{2-}$	1200.0	0.149	120.0
$Zn^{2+} - Zn^{2+}$	0.0	0.0	0.0
$Zn^{2+} - S^{2-}$	613.356	0.399	0.0
K (eV $\cdot rad^{-2}$)		0.778	
θ_0 (deg)		109.47	

[1] N. Alem, Q. M. Ramasse, C. R. Seabourne, O. V. Yazyev, K. Erickson, M. C. Sarahan, C. Kisielowski, A. J. Scott, S. G. Louie, and A. Zettl, Phys. Rev. Lett., **109**, 205502 (2012).

[2] D. J. Binks and R. W. Grimes, Solid State Commun., **89**, 921 (1994).

[3] Z. Chen, Z. Yu, P. Lu, and Y. Liu, Physica B: Condensed Matter, **404**, 4211 (2009).

[4] S. Dai, M. L. Dunn, and H. S. Park, Nanotechnology, **21**, 445707 (2010).

[5] M. P. Tosi, Solid State Phys., **16**, 1 (1964).

[6] C. R. A. Catlow and W. C. Mackrodt, *Computer simulation of solids* (Springer, 1982).

[7] S. Plimpton, J. Comput. Phys., **117**, 1 (1995).

[8] E. E. Gdoutos, R. Agrawal, and H. D. Espinosa, Int. J. Numer. Meth. Eng., **84**, 1541 (2010).

[9] S. Hamad, S. Cristol, and C. R. A. Catlow, J. Phys. Chem. B, **106**, 11002 (2002).